



UDC 621.762.34

<https://doi.org/10.17073/1997-308X-2025-2-15-23>Research article  
Научная статья

## Optimization of powder mixing parameters for the Al–Sn–Pb system for use in selective laser melting

K. O. Akimov<sup>1</sup>, A. L. Skorentsev<sup>1, 2</sup>, N. M. Rusin<sup>1</sup>, V. E. Likharev<sup>1, 2</sup>,  
A. Yu. Nikonov<sup>1, 3</sup>, A. I. Dmitriev<sup>1, 3✉</sup>

<sup>1</sup> Institute of Strength Physics and Materials Science  
of the Siberian Branch of the Russian Academy of Sciences

2/4 Akademichesky Prospekt, Tomsk 634055, Russia

<sup>2</sup> National Research Tomsk Polytechnic University

30 Lenina Prospekt, Tomsk 634050, Russia

<sup>3</sup> National Research Tomsk State University

36 Lenina Prospekt, Tomsk 634050, Russia

dmitr@ispms.ru

**Abstract.** This study presents the results of research on optimizing powder mixing parameters for the Al–15Sn–5Pb (vol. %) system for application in selective laser melting technology. The primary focus is on ensuring the uniform distribution of soft-phase particles (Sn and Pb), which is essential for obtaining products with a homogeneous structure and improved tribological properties. The initial materials used in the study were aluminum (ASD-1), tin (PO-1), and lead (PS-1) powders. Before mixing, the powders were sieved using mesh sizes ranging from 50 to 25 µm. The sieved powders had a nearly spherical shape and good flowability characteristics (less than 25 s / 50 g). The effect of mixing time on the homogeneity of the powder mixture was studied using the discrete element method and a modified Hertz–Mindlin model. The obtained mixtures were analyzed using X-ray phase analysis, micro-X-ray spectral analysis, and graphical analysis methods. Subsequent experimental validation confirmed the reliability of numerical calculations and enabled the assessment of optimal mixing parameters. It was established that the optimal mixing time for achieving a uniform distribution of the initial powder particles falls within the range of 60 to 120 min. It was also found that the complex motion pattern of a *Turbula*-type mixer reduces the impact of gravitational segregation, thereby improving the uniform distribution of soft-phase particles (Sn + Pb). The proposed approach can be used for developing new powder preparation methods for additive manufacturing technologies and for creating composite materials with enhanced performance characteristics.

**Keywords:** selective laser melting (SLM), aluminum alloys, antifriction alloys, discrete elements method, mixing

**Acknowledgements:** This study was supported by the Russian Science Foundation [Grant No. 24-79-10099], <https://ias.rscf.ru/user/doc/a.w.p.2024.98.legacy/182272>.

**For citation:** Akimov K.O., Skorentsev A.L., Rusin N.M., Likharev V.E., Nikonov A.Yu., Dmitriev A.I. Optimization of powder mixing parameters for the Al–Sn–Pb system for use in selective laser melting. *Powder Metallurgy and Functional Coatings*. 2025;19(2):15–23. <https://doi.org/10.17073/1997-308X-2025-2-15-23>

# Оптимизация параметров смещивания порошков системы Al-Sn-Pb для использования при селективном лазерном сплавлении

К. О. Акимов<sup>1</sup>, А. Л. Скоренцев<sup>1, 2</sup>, Н. М. Русин<sup>1</sup>, В. Е. Лихарев<sup>1, 2</sup>,  
А. Ю. Никонов<sup>1, 3</sup>, А. И. Дмитриев<sup>1, 3</sup> 

<sup>1</sup> Институт физики прочности и материаловедения Сибирского отделения Российской академии наук  
Россия, 634055, г. Томск, пр-т Академический, 2/4

<sup>2</sup> Национальный исследовательский Томский политехнический университет  
Россия, 634050, г. Томск, пр-т Ленина, 30

<sup>3</sup> Национальный исследовательский Томский государственный университет  
Россия, 634050, г. Томск, пр-т Ленина, 36

 dmitr@ispms.ru

**Аннотация.** В работе представлены результаты исследования по оптимизации параметров смещивания порошков системы Al-15Sn-5Pb (об. %) для применения их в технологии селективного лазерного сплавления. Основное внимание уделено обеспечению равномерного распределения частиц мягкой фазы (Sn и Pb), необходимого для получения изделий с однородной структурой и улучшенными триботехническими свойствами. В качестве исходных материалов использовались порошки алюминия (АСД-1), олова (ПО-1) и свинца (ПС-1). Перед смещиванием проводился их просев через сита с размерами ячеек от 50 до 25 мкм. Просеянные порошки имели форму, близкую к сферической, и хорошие характеристики текучести (менее 25 с / 50 г). С использованием метода дискретных элементов и модифицированной модели Герца-Миндлина изучено влияние времени смещивания на степень гомогенности порошковой смеси. Исследования полученных смесей проводились с помощью рентгенофазового, микрорентгеноспектрального и графического методов анализа. Последующая экспериментальная валидация подтвердила достоверность результатов численных расчетов и позволила оценить оптимальные параметры смещения. Установлено, что оптимальное время смещивания, позволяющее получить равномерное распределение исходных порошковых частиц, находится в интервале от 60 до 120 мин. Обнаружено, что сложный характер движения смесителя типа «Турбула» снижает влияние гравитационной сегрегации, улучшая равномерность распределения частиц мягкой фазы (Sn + Pb). Предложенный подход может быть использован для разработки новых методик подготовки порошков для аддитивных технологий и создания композиционных материалов с улучшенными эксплуатационными характеристиками.

**Ключевые слова:** селективное лазерное сплавление (СЛС), алюминиевые сплавы, антифрикционные сплавы, метод дискретных элементов, перемешивание

**Благодарности:** Работа выполнена при финансовой поддержке Российского научного фонда [грант № 24-79-10099], <https://ias.rscf.ru/user/doc/a.w.p.2024.98.legacy/182272>.

**Для цитирования:** Акимов К.О., Скоренцев А.Л., Русин Н.М., Лихарев В.Е., Никонов А.Ю., Дмитриев А.И. Оптимизация параметров смещивания порошков системы Al-Sn-Pb для использования при селективном лазерном сплавлении. *Известия вузов. Порошковая металлургия и функциональные покрытия*. 2025;19(2):15–23.  
<https://doi.org/10.17073/1997-308X-2025-2-15-23>

## Introduction

The growing demand for high-performance anti-friction materials in advanced engineering applications is driving the development of new metallic powder compositions designed to produce components with enhanced tribological properties [1–3]. This trend, combined with the rapid adoption of additive manufacturing technologies, imposes stricter requirements on the preparation of multicomponent powder mixtures. The extreme nonequilibrium conditions of the selective laser melting (SLM) process, characterized by intense heating ( $>10^6$  K/s) and cooling rates ( $10^3$ – $10^8$  K/s), necessitate a high degree of homogeneity in the ini-

tial powder mixture, as any inhomogeneities can lead to structural defects and anisotropy, ultimately degrading the properties of the final components [4; 5].

Aluminum alloys are among the most widely used materials across various industries due to their unique combination of strength and low density, enabling the production of lightweight yet durable machine components. The integration of aluminum alloys into 3D printing technologies further enhances their appeal by providing additional design flexibility in terms of shape and structure [6]. The Al-15Sn-5Pb (vol. %) system is a specialized alloy intended for anti-friction applications, such as sliding bearings, where tin and

lead act as solid lubricants, reducing wear during frictional contact [7–9]. However, the tendency of these inclusions to segregate during both powder mixing and solidification in the 3D printing process necessitates stringent control over the composition of the powder mixture to ensure their uniform distribution in the final product [10]. Additionally, the relatively low evaporation temperature of lead ( $1749^{\circ}\text{C}$ ) compared to the typical process temperatures of aluminum alloy SLM ( $>2000^{\circ}\text{C}$ ) requires precise energy input control to prevent selective evaporation [11].

Mixing powders with significant density differences poses a fundamental challenge [12]. In the Al–15Sn–5Pb system, where the density ratio of lead to aluminum is approximately 4.2:1.0, this issue becomes particularly pronounced. Traditional drum mixers, which operate mainly by gravitational forces, tend to promote segregation rather than effective mixing in such systems, as denser lead and tin particles naturally migrate downward. This results in localized inhomogeneities in the powder mixture, which is critical for its subsequent use in SLM [13]. One potential solution to this problem is the use of a *Turbula*-type mixer manufactured by Vibrotechnik (Russia), which combines rotational and translational motion in a rhythmic three-dimensional pattern. This complex motion induces intense mixing conditions that counteract gravitational effects, thereby reducing segregation driven by density differences. The powder layer periodically experiences near-weightlessness, followed by abrupt directional changes, which help prevent agglomeration.

The objective of this study was to evaluate the effectiveness of the modified Hertz–Mindlin model in predicting the quality of the resulting powder mixture composed of components with significant density variations, as well as to determine the optimal mixing parameters for the Al–15Sn–5Pb system using a *Turbula*-type mixer. The research focused on identifying the minimum mixing time required to achieve compositional homogeneity sufficient for the successful application of powder mixtures with large density differences in the SLM process.

## Materials and methods

The experiments were conducted using aluminum (ASD-1), tin (PO-1), and lead (PS-1) powders. The powders were sieved through meshes with an upper cell size limit of 50  $\mu\text{m}$  and a lower limit of 25  $\mu\text{m}$ .

Analysis of several scanning electron microscopy (SEM) images revealed that the average particle size of all studied powders was 30  $\mu\text{m}$  (Fig. 1), with a size distribution approximating a normal distribution. The aluminum powder particles had a spherical shape,

whereas the tin and lead powders exhibited both spherical and dumbbell-like morphologies.

Additionally, powder flowability was analyzed using funnels with outlet diameters of 2.5 mm (tin, lead) and 5 mm (aluminum) according to GOST 20899–98 (ISO 4490–78). Measurements of the natural repose angle showed that its value for all three powders was approximately 30°. The flowability of the tin and lead powders did not exceed 20 s/50 g, while that of aluminum was 26 s/50 g, indicating their suitability for SLM technology.

Mixing simulations were performed using the discrete element method (DEM) with the Altair EDEM software package (Altair Engineering, USA). The par-

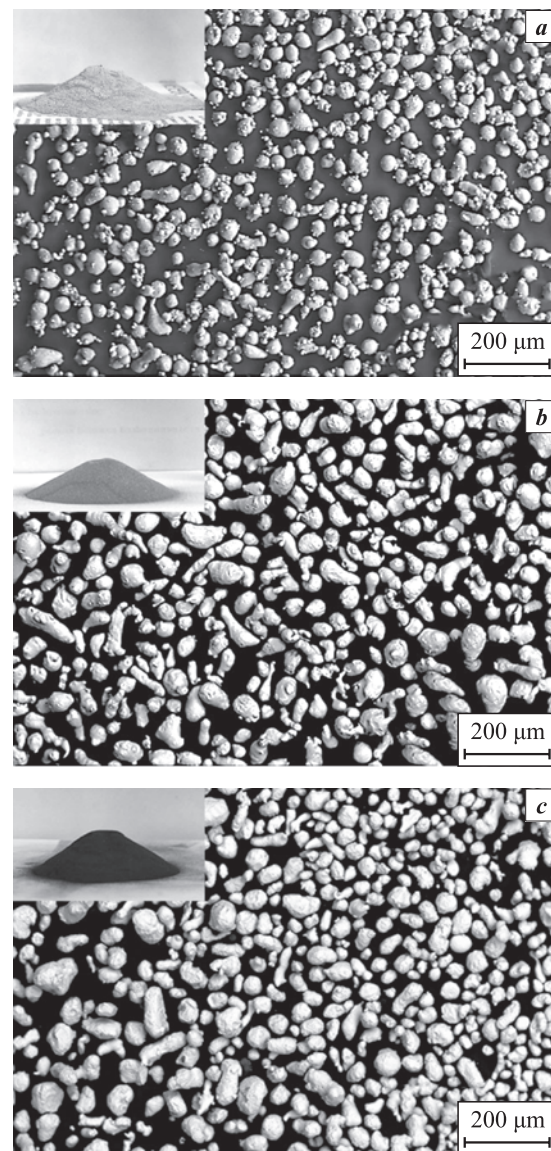


**Fig. 1.** SEM images of Al (a), Sn (b), and Pb (c) powders before mixing in a *Turbula* mixer

**Рис. 1.** РЭМ-изображения порошков Al (а), Sn (б) и Pb (с) перед смещиванием в смесителе типа «Турбула»

ticle-to-particle and particle-to-wall interactions were described by the Hertz–Mindlin model, modified according to the Johnson–Kendall–Roberts (JKR) theory [14; 15]. This contact interaction model is widely used in powder mixing simulations to account for adhesion forces [16–21]. To accelerate computational time, model scaling was applied, reducing the container size and powder mass by a factor of three.

The physical parameters of the powders used in the model are presented in Tables 1 and 2. The friction and restitution coefficients were averaged based on data from various sources [22–26]. For Sn and Pb friction pairs, the friction coefficients were taken from similar bearing steels with comparable properties.

To analyze the variation in the tin and lead powder content during mixing, the container volume was conditionally divided into 28 cells, where the fraction of each metal's particles was assessed using the formula  $N_{ij}/V_{ij}$ , where  $N_{ij}$  is the number of Sn and Pb particles,  $V_{ij}$  is the cell volume, and  $i$  and  $j$  are the cell indices along the  $X$  and  $Y$  axes, respectively (Fig. 2).

In a *Turbula*-type mixer, the powder mixture was blended at a container rotation speed of 30 rpm. The mixing duration varied within the range of  $\tau = 10\text{--}240$  min. From the obtained mixtures, 10 compacts were produced by pressing, with the powder for each compact being taken from different parts of the container.

An initial analysis of the composition of the initial components in the powder mixture was performed using X-ray phase analysis with a DRON-8 diffractometer (NPP Burevestnik, Russia) in  $\text{Cu}K_\alpha$  radiation ( $\lambda = 1.5406 \text{ \AA}$ ) over a 20 range of 10–110°.

For metallographic studies, cross-sections of the compacts along their diameters were examined.

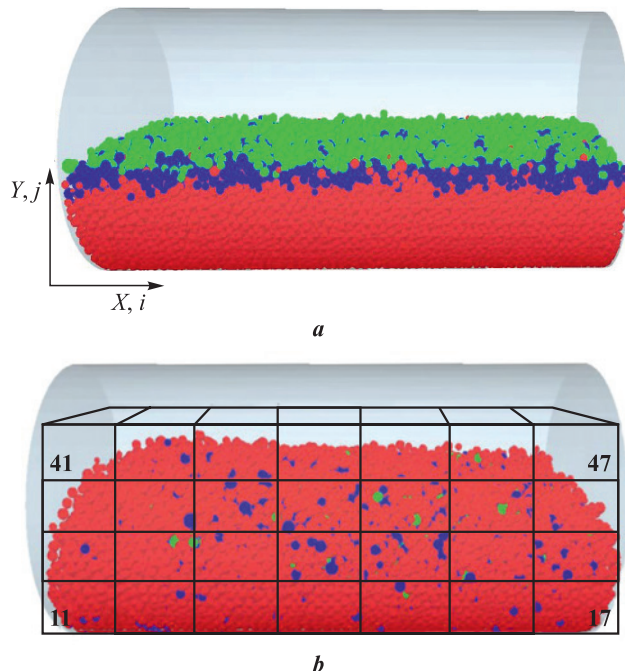


**Fig. 2.** Container model with powders at the beginning (a) and after 3 h of mixing (b)

The first digit in Figure b corresponds to the  $i$  index,  
and the second to  $j$  index

Al is highlighted in red, Sn in blue, and Pb in green

**Рис. 2.** Модель контейнера с порошками в начале (а)

и после 3 ч перемешивания (б)

Первая цифра на рисунке б соответствует индексу  $i$ ,  
вторая –  $j$

Al выделен красным цветом, Sn – синим, Pb – зеленым

The microstructural analysis of the obtained compacts, as well as the elemental composition assessment, was conducted using a LEO EVO 50 scanning electron microscope (Carl Zeiss, Germany) equipped with an energy-dispersive X-ray spectroscopy (EDS)

**Table 1. Physical parameters of powders used in the simulation**

**Таблица 1. Физические параметры порошков, заложенные в моделирование**

Powder	Particle diameter, m	Particle density, kg/m <sup>3</sup>	Poisson's ratio	Shear modulus, Pa·10 <sup>9</sup>	Particle mass, kg	Number of particles, pcs
Al	$0.001 \pm 0.0003$	2700	0.33	26.30	0.283	22,391
Sn	$0.001 \pm 0.0003$	7300	0.44	12.15	0.074	4,203
Pb	$0.001 \pm 0.0003$	11 300	0.43	4.90	0.143	1,418

**Table 2. Friction and restitution coefficients of the simulated powders**

**Таблица 2. Коэффициенты трения и реституции моделируемых порошков**

Parameter	Friction pair								
	Al–Al	Sn–Sn	Pb–Pb	Al–Sn	Al–Pb	Sn–Pb	Al–steel	Sn–steel	Pb–steel
Static friction coefficient	1.1	0.74	0.9	0.5	0.5	1.4	0.50	0.40	0.30
Rolling friction coefficient	0.3	0.20	0.2	0.2	0.2	0.5	0.05	0.05	0.05
Restitution coefficient	0.6	0.50	0.4	0.5	0.5	0.5	0.60	0.60	0.60

module. The graphical analysis of SEM images of the compact cross-sections was performed using ImageJ software (National Institutes of Health, USA).

## Results and discussion

### Simulation

The simulation results for the number of tin and lead particles in different areas of the container over 3 h of mixing, approximated by logarithmic dependencies, are presented in Fig. 3. It was found that at a mixing duration ( $\tau$ ) of up to 30 min, the majority of both lead and tin particles remain predominantly in the upper layers of the powder mixture, despite the complex motion pattern of the container during the process. This may be attributed to the formation of temporary agglomerates of Sn and Pb particles, as these powders exhibit a high tendency toward adhesion due to their lower hardness and high plasticity compared to aluminum, leading to the formation of more stable contacts. As  $\tau$  increases to 60 min, the dependencies of Sn and Pb particle content in different cells converge within the 4–6 % range and nearly equalize at 180 min.

Based on these results, it can be assumed that to obtain a near-homogeneous Al–15Sn–5Pb mixture, the minimum mixing time in the *Turbula* mixer should be 60 min at a container rotation speed of 30 rpm.

### Experiment

A typical diffractogram of a compact made from the Al–15Sn–5Pb mixture and the dependence of the soft-phase (Sn + Pb) content on the mixing time,

calculated using the corundum number method, are presented in Fig. 4. It can be observed that at short mixing times, the soft-phase content is lower (15 vol. %), with significant variations (6 %) in its values (Fig. 4, *b*). These data partially confirm the simulation results, indicating the presence of soft-phase particle agglomerates. The expected tin and lead content levels in the mixture are reached after 60 min of mixing, confirming the reliability of the applied numerical model. In the 120–180 min time range, the dependence acquires a linear character, and the variation in soft-phase element content does not exceed 2 %.

The results of SEM studies, presented in Fig. 5, indicate that at short mixing times ( $\tau = 10$ –60 min), an uneven distribution of soft-phase particles is observed, with large agglomerates of various shapes reaching 300  $\mu\text{m}$  in size. The use of such powder mixtures in SLM would likely result in large defects due to local inhomogeneities in the initial powder distribution. At  $\tau = 120$ –240 min, tin and lead become more evenly distributed across the polished section surface, and the size of soft-phase agglomerates decreases. Completely eliminating these agglomerates is not feasible due to the inherent tendency of these powders to adhere. However, at this stage, the powder mixtures can be considered suitable for SLM technology.

The EDS analysis results of the compact element composition are presented in Table 3. According to the data, even at short mixing times, the mixture contains Sn and Pb levels close to the target composition. However, due to inhomogeneous distribution within the powder volume, a significant deviation from the mean is observed in different sections of the com-

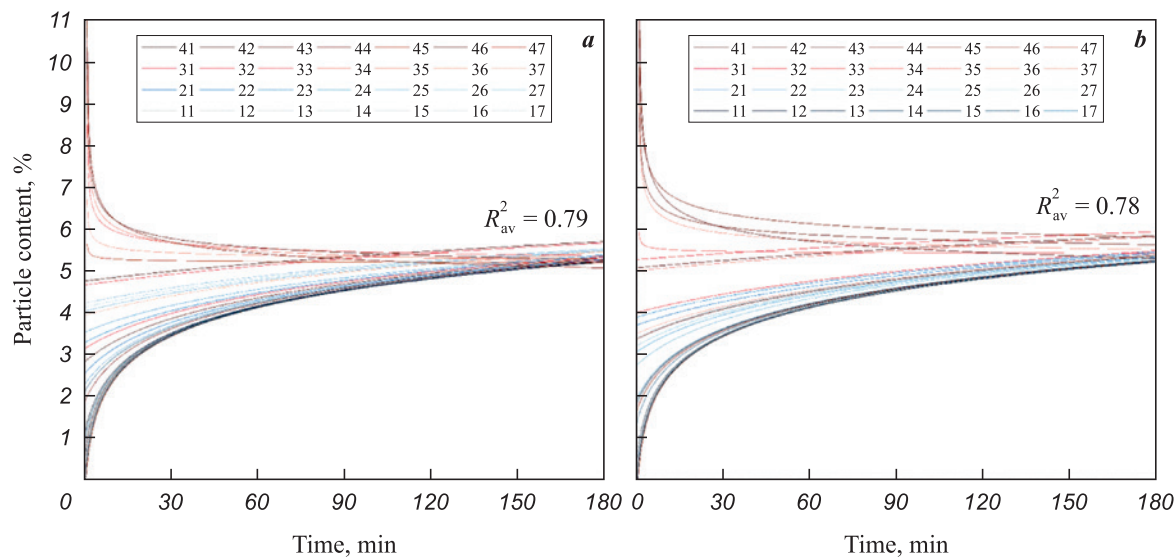


**Fig. 3.** Dependences of the content of Sn (a) and Pb (b) particles in the cells (11–47) of the container on the mixing time

**Рис. 3.** Зависимости содержания частиц Sn (а) и Pb (б) в ячейках (11–47) контейнера от времени перемешивания

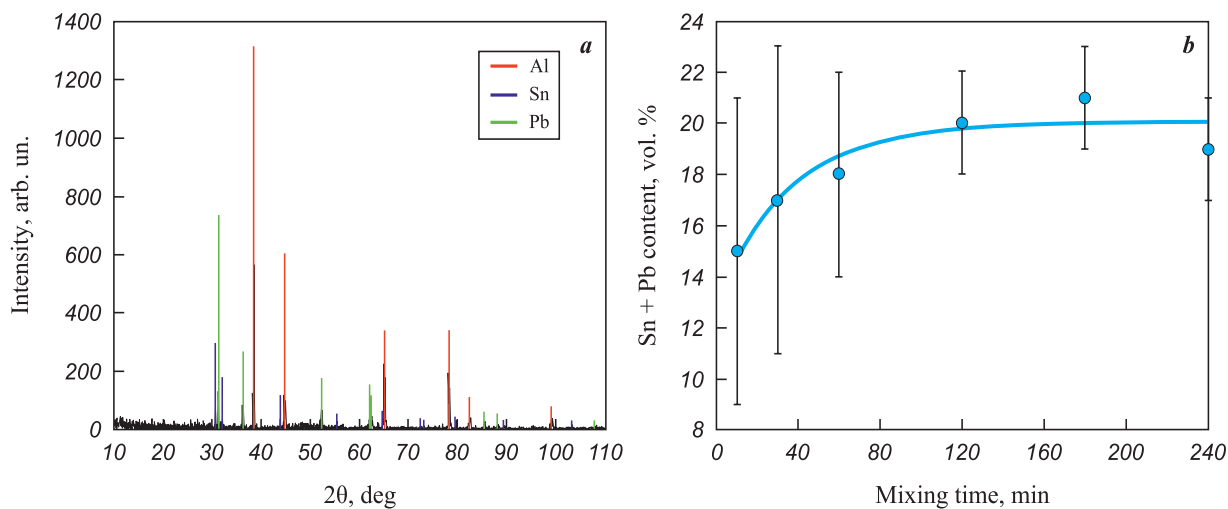


**Fig. 4.** Typical diffractogram of the Al–15Sn–5Pb mixture (a)  
and dependence of the soft-phase (Sn + Pb) content on the mixing time (b)

**Рис. 4.** Типичная дифрактограмма смеси состава Al–15Sn–5Pb (a)  
и зависимость содержания мягкой фазы Sn + Pb от времени перемешивания (b)

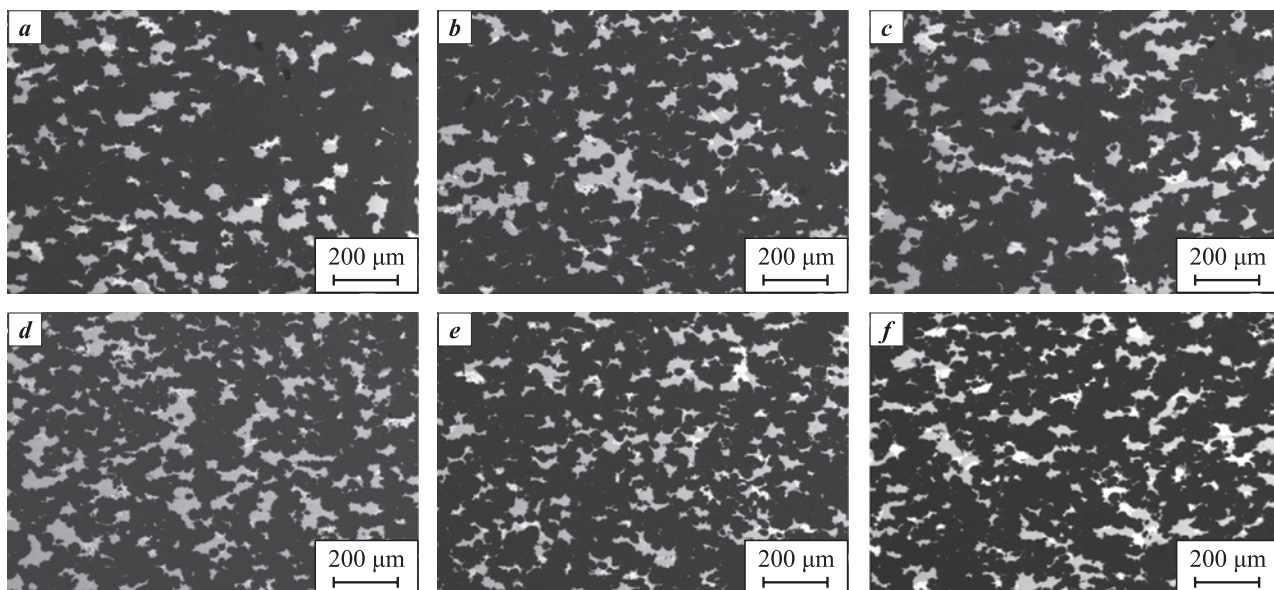


**Fig. 5.** Typical SEM images of cross-sections of powder compacts  
obtained from mixtures after 10 (a), 30 (b), 60 (c), 120 (d), 180 (e), and 240 min (f) of mixing  
Dark phase – Al, bright phases – Sn and Pb

**Рис. 5.** Типичные РЭМ-снимки поперечных сечений исследуемых компактов из порошковых смесей,  
полученных после перемешивания в течение 10 (a), 30 (b), 60 (c), 120 (d), 180 (e) и 240 мин (f)  
Темная фаза – Al, светлые – Sn и Pb

pacts. After 60 min of mixing, these deviations are reduced by approximately a factor of two, indicating the breakdown of large agglomerates. Mixing for 120 min or longer further decreases the deviation from the average element content within different compact sections to  $\approx 2\%$ , suggesting that the elements have reached a sufficiently homogeneous distribution throughout the volume.

In addition to EDS analysis, graphical analysis of SEM images was conducted using ImageJ software to assess the quantity and size of soft-phase (Sn + Pb) agglomerates (Fig. 6). The fraction of lead and tin was determined based on the area occupied by these particles. For each  $\tau$  value, 10 images per compact were analyzed.

The analysis revealed that the tin and lead content follows an approximately linear trend. However,

**Table 3. Elemental content in powder compacts depending on mixing time**

**Таблица 3. Содержание элементов в компактах из порошковых смесей в зависимости от времени перемешивания**

$\tau$ , min	Content, vol. %		
	Al	Sn	Pb
10	81 ± 8	15 ± 8	4 ± 3
30	80 ± 5	15 ± 6	5 ± 3
60	80 ± 4	15 ± 4	5 ± 2
120	80 ± 2	16 ± 2	4 ± 1
180	80 ± 2	16 ± 2	4 ± 1
240	80 ± 2	16 ± 2	4 ± 1

at short mixing times, as observed in the EDS results, there is a high relative deviation in particle distribution within the volume ( $\pm 6\%$ ), which decreases to 1 % as  $\tau$  increases. Despite the relative deviation reduction occurring as early as  $\tau = 60$  min, it is also important to consider the size of Sn and Pb agglomerates. The trend in agglomerate area reduction follows a linear downward pattern. With an increase in mixing duration, the agglomerate area decreases by approximately 35 %, from 1400 to  $900 \mu\text{m}^2$  at  $\tau = 10$  and 240 min, respectively. At the same time, the deviation value also decreases from 16 to 10 %, but remains relatively high. This is likely due to the formation of agglomerates within the internal volume of the powder mixture, which, lacking direct contact with the container walls, were more resistant to breakdown during mixing.

These findings indicate not only an improvement in mixture homogeneity within a relatively short period ( $\tau = 60$ –120 min) but also the effectiveness of the modified Hertz–Mindlin model for simulating the mixing process in powder systems with significant density differences between their components.

## Conclusions

Based on the obtained results, the following conclusions can be drawn.

1. The complex motion pattern of the *Turbula* mixer ensures effective mixing of the Al–15Sn–5Pb powder system, reducing the impact of gravitational segregation and improving the uniformity of soft-phase (Sn + Pb) particle distribution. This allows for its further application in selective laser melting (SLM) technology.

2. The discrete element method with the modified Hertz–Mindlin model demonstrated high reliability in predicting the homogeneity evolution of powder mixtures, which was confirmed by experimental data.

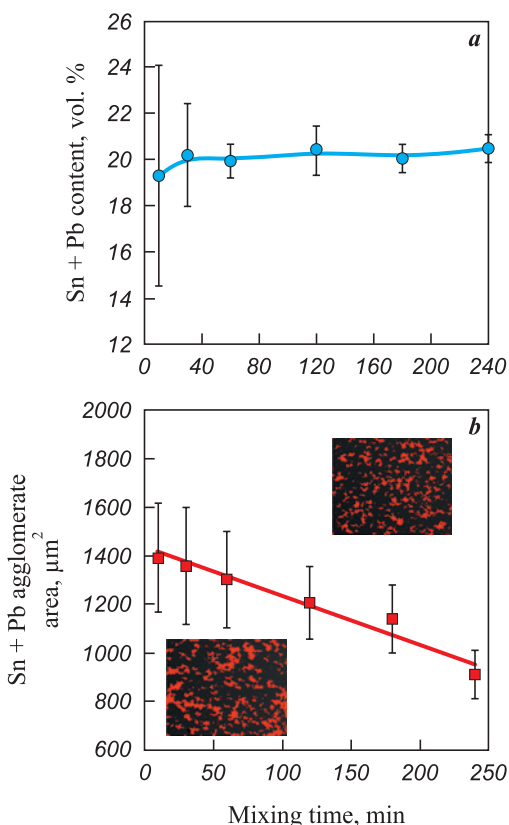


**Fig. 6. Dependences of the content (a) and agglomerate size (b) of the soft phase (Sn + Pb) on the mixing time in the *Turbula* mixer**

**Рис. 6. Зависимости содержания (а) и размеров агломератов (б) мягкой фазы (Sn + Pb) от времени перемешивания в смесителе «Турбула»**

3. It was established that reducing the size of soft-phase (Sn + Pb) agglomerates and minimizing component distribution deviations occur at a mixing time of 60 to 120 min, making this interval recommended for practical applications.

4. The obtained results can be utilized to improve powder preparation quality for additive manufacturing technologies and to develop new powder materials with enhanced performance characteristics.

## References / Список литературы

- Ralls A., Merbin J., Noud J., Lopez J., LeSourd Kasey, Napier I., Hallas N., Menezes P. Tribological, corrosion, and mechanical properties of selective laser melted steel. *Metals*. 2022;12(10):1732. <https://doi.org/10.3390/met12101732>
- Yang G., Zhang J., Xie H., Li F., Huang Z., Yuan G., Zhang J., Jia Q., Zhang H., Yeprem H.A., Zhang S. Preparation of  $\text{B}_4\text{C}/\text{Al}$  composites via selective laser melting and their tribological properties. *Materials*. 2022;15:8340. <https://doi.org/10.3390/ma15238340>
- Rusin N.M., Akimov K.O., Skorentsev A.L., Dmitriev A.I. Influence of laser power during laser powder bed fusion on the structure and properties of Al–40Sn alloy prepared

- from a mixture of elemental powders. *Journal of Alloys and Compounds*. 2025;1013:178647.  
<https://doi.org/10.1016/j.jallcom.2025.178648>
4. Mukherjee T., DebRoy T. A digital twin for rapid qualification of 3D printed metallic components. *Applied Materials Today*. 2019;14:59–65.  
<https://doi.org/10.1016/j.apmt.2018.11.003>
  5. Han Tianyi, Chen Jiaying, Wei Zongfan, Qu Nan, Liu Y., Yand D., Zhao S., Lai Z., Jiang M., Zhu J. Effect of cooling rate on microstructure and mechanical properties of AlCrFe<sub>2</sub>Ni<sub>2</sub> medium entropy alloy fabricated by laser powder bed fusion. *Journal of Materials Research and Technology*. 2023;25:4063–4073.  
<https://doi.org/10.1016/j.jmrt.2023.06.241>
  6. Wang Z., Ummethala R., Singh N., Tang S., Suryanarayana C., Eckert J., Prashanth K.G. Selective laser melting of aluminum and its alloys. *Materials*. 2020;13:4564.  
<https://doi.org/10.3390/ma13204564>
  7. Rusin N.M., Skorentsev A.L., Akimov K.O. Mechanical properties of sintered Al–Sn–Fe alloys. *Physical Mesomechanics*. 2024;27(1):69–78.  
<https://doi.org/10.1134/S1029959924010077>
  8. Confalonieri C., Gariboldi E. Al–Sn miscibility gap alloy produced by power bed laser melting for application as phase change material. *Journal of Alloys and Compounds*. 2021;881:160569.  
<https://doi.org/10.1016/j.jallcom.2021.160596>
  9. Rusin N.M., Skorentsev A.L., Akimov K.O. Al–40Sn alloy produced by selective laser melting of elemental powder mixtures. *Physics of Metals and Metallography*. 2023;124(9):908–915.  
<https://doi.org/10.1134/S0031918X23601476>
  10. Guo Z., Jie J., Liu S., Yue S., Zhang Y., Li T. Solidification characteristics and segregation behavior of Cu–15Ni–8Sn alloy. *Metallurgical and Materials Transactions A*. 2020;51:1229–1241.  
<https://doi.org/10.1007/s11661-019-05609-y>
  11. Shi G., Zhang R., Cao Y., Yang G. A review of the vaporization behavior of some metal elements in the LPBF process. *Micromachines*. 2024;15:846.  
<https://doi.org/10.3390/mi15070846>
  12. Hogg R. Mixing and segregation in powders: Evaluation, mechanisms and processes. *KONA Powder and Particle Journal*. 2009;27:3–17.  
<https://doi.org/10.14356/kona.2009005>
  13. Vock S., Klöden B., Kirchner A., Weißgärber T., Kieback B. Powders for powder bed fusion: A review. *Progress in Additive Manufacturing*. 2019;4:383–397.  
<https://doi.org/10.1007/s40964-019-00078-6>
  14. Hertz H. On the contact of elastic solids. *Journal für die Reine und Angewandte Mathematik*. 1882;92:156–171.
  15. Johnson K.L., Kendall K., Roberts A. Surface energy and the contact of elastic solids. *Proceedings of the Royal Society A*. 1971;324:301–313.
  16. Li J., Peng F., Li H., Ru Z., Fu J., Zhu W. Material evaluation and dynamic powder deposition modeling of PEEK/CF composite for laser powder bed fusion process. *Polymers*. 2023;15:2863.  
<https://doi.org/10.3390/polym15132863>
  17. Yan W., Qian Y., Ge W., Lin S., Liu W.K., Lin F., Wagner G.J. Meso-scale modeling of multiple-layer fabrication process in selective electron beam melting. *Materials and Design*. 2018;14:210–219.  
<https://doi.org/10.1016/j.matdes.2017.12.031>
  18. Yeom S.B., Ha E.-S., Kim M.-S., Jeong S.H., Hwang S.-J., Choi D.H. Application of the discrete element method for manufacturing process simulation in the pharmaceutical industry. *Pharmaceutics*. 2019;11:414.  
<https://doi.org/10.3390/pharmaceutics11080414>
  19. Horabik J., Molenda M. Parameters and contact models for DEM simulations of agricultural granular materials: A review. *Biosystems Engineering*. 2016;147:206–225.  
<https://doi.org/10.1016/j.biosystemseng.2016.02.017>
  20. Pantaleev S., Yordanova S., Janda A., Marigo M., Jin Y.O. An experimentally validated DEM study of powder mixing in a paddle blade mixer. *Powder Technology*. 2017;311:287–302.  
<https://doi.org/10.1016/j.powtec.2016.12.053>
  21. Marigo M., Cairns D.L., Davies M., Ingram A., Stitt E.H. Developing mechanistic understanding of granular behaviour in complex moving geometry using the discrete element method. Part B. Investigation of flow and mixing in the Turbula® mixer. *Powder Technology*. 2011;212(1):1724.  
<https://doi.org/10.1016/j.powtec.2011.04.009>
  22. Totten G.E. ASM Handbook. Vol. 18. Friction, lubrication, and wear technology. Ohio: ASM International, 2017. 1091 p.
  23. Bajpai A., Saxena P., Kunze K. Tribomechanical characterization of carbon fiber-reinforced cyanate ester resins modified with fillers. *Polymers*. 2020;12:1725.  
<https://doi.org/10.3390/polym12081725>
  24. Bowden F.P., Tabor D. The friction and lubrication of solids. Oxford: University Press, 2001. 424 p.
  25. Anurev V.I. Handbook of the mechanical engineer-designer. Vol. 1. Moscow: Mashinostroenie, 2001. 920 p. (In Russ.).  
 Анурев В.И. Справочник конструктора-машиностроителя. Т. 1. М.: Машиностроение, 2001. 920 с.
  26. Blanter M.S., Golovin I. S., Neuhäuser H., Sinning H.-R. Internal friction in metallic materials: A Handbook. Berlin: Springer, 2007. 520 p.

### Information about the Authors

**Kirill O. Akimov** – Cand. Sci. (Eng.), Research Associate of the Laboratory of Powder Materials Consolidation Physics, Institute of Strength Physics and Materials Science of the Siberian Branch of Russian Academy of Sciences (ISPMS SB RAS)

ID ORCID: 0000-0002-3204-250X

E-mail: akimov\_ko@ispms.ru

### Сведения об авторах

**Кирилл Олегович Акимов** – к.т.н., науч. сотрудник лаборатории физики консолидации порошковых материалов, Институт физики прочности и материаловедения Сибирского отделения Российской академии наук (ИФПМ СО РАН)

ID ORCID: 0000-0002-3204-250X

E-mail: akimov\_ko@ispms.ru

**Alexander L. Skorentsev** – Cand. Sci. (Eng.), Research Associate of the Laboratory of Powder Materials Consolidation Physics, ISPMS SB RAS; Engineer of the Department of Experimental Physics, School of Nuclear Engineering, National Research Tomsk Polytechnic University (TPU)

 **ORCID:** 0000-0003-2506-9437

 **E-mail:** skoralexan@ispms.ru

**Nikolay M. Rusin** – Cand. Sci. (Eng.), Senior Research Scientist of the Laboratory of Powder Materials Consolidation Physics, ISPMS SB RAS

 **ORCID:** 0000-0002-7537-7895

 **E-mail:** rusinnm@ispms.ru

**Vadim E. Likharev** – Engineer of the Laboratory of Powder Materials Consolidation Physics, ISPMS SB RAS; Student of the engineering school of new production materials, TPU

 **ORCID:** 0009-0002-4713-3663

 **E-mail:** vel6@tpu.ru

**Anton Yu. Nikonov** – Cand. Sci. (Phys.Math.), Research Associate of the Laboratory of Computer-Aided Design of Materials, ISPMS SB RAS; Associate Professor of the Department of Physics of Metals, Faculty of Physics, National Research Tomsk State University (TSU)

 **ORCID:** 0000-0002-0980-0317

 **E-mail:** anickonoff@ispms.ru

**Andrey I. Dmitriev** – Dr. Sci. (Phys.Math.), Principal Researcher of the Laboratory of Powder Materials Consolidation Physics, ISPMS SB RAS; Professor of the Department of Physics of Metals, Faculty of Physics, TSU

 **ORCID:** 0000-0002-2823-578X

 **E-mail:** dmitr@ispms.ru

**Александр Леонидович Скоренцев** – к.т.н., науч. сотрудник лаборатории физики консолидации порошковых материалов, ИФПМ СО РАН; инженер отделения экспериментальной физики инженерной школы ядерных технологий, Национальный исследовательский Томский политехнический университет (ТПУ)

 **ORCID:** 0000-0003-2506-9437

 **E-mail:** skoralexan@ispms.ru

**Николай Мартемьянович Русин** – к.т.н., ст. науч. сотрудник лаборатории физики консолидации порошковых материалов, ИФПМ СО РАН

 **ORCID:** 0000-0002-7537-7895

 **E-mail:** rusinnm@ispms.ru

**Вадим Евгеньевич Лихарев** – инженер лаборатории физики консолидации порошковых материалов, ИФПМ СО РАН; студент инженерной школы новых производственных материалов, ТПУ

 **ORCID:** 0009-0002-4713-3663

 **E-mail:** vel6@tpu.ru

**Антон Юрьевич Никонов** – к.ф.-м.н., науч. сотрудник лаборатории компьютерного конструирования материалов, ИФПМ СО РАН; доцент кафедры физики металлов физического факультета, Национальный исследовательский Томский государственный университет (ТГУ)

 **ORCID:** 0000-0002-0980-0317

 **E-mail:** anickonoff@ispms.ru

**Андрей Иванович Дмитриев** – д.ф.-м.н., гл. науч. сотрудник лаборатории физики консолидации порошковых материалов, ИФПМ СО РАН; профессор кафедры физики металлов физического факультета, ТГУ

 **ORCID:** 0000-0002-2823-578X

 **E-mail:** dmitr@ispms.ru

### Contribution of the Authors

### Вклад авторов

**K. O. Akimov** – formulation of the research problem, analysis of results using SEM, modeling, manuscript preparation.

**A. L. Skorentsev** – preparation of samples for SEM, discussion of results.

**N. M. Rusin** – X-ray phase analysis, discussion of results.

**V. E. Likharev** – preparation of the powder mixtures.

**A. Yu. Nikonov** – formulation of the simulation problem, discussion of the results.

**A. I. Dmitriev** – overall supervision of the study, analysis of simulation results, discussion of results, manuscript editing.

**К. О. Акимов** – постановка задачи, анализ результатов с использованием РЭМ, моделирование, написание статьи.

**А. Л. Скоренцев** – подготовка образцов для РЭМ, обсуждение результатов.

**Н. М. Русин** – рентгенофазовый анализ, обсуждение результатов.

**В. Е. Лихарев** – подготовка порошковых смесей.

**А. Ю. Никонов** – постановка задачи моделирования, обсуждение результатов.

**А. И. Дмитриев** – общее руководство работой, анализ результатов моделирования, обсуждение результатов, редактирование рукописи.

Received 23.01.2025

Revised 12.03.2025

Accepted 13.03.2025

Статья поступила 23.01.2025 г.

Доработана 12.03.2025 г.

Принята к публикации 13.03.2025 г.